

Original Research Article**A Comprehensive Miss Distance Analysis of Single-Lag True Proportional Navigation**S. H. Jalali-Naini^{1*} , Rahim Asadi , Amir Hossein Mirzaei

1-2-3 Department of Mechanical Engineering, Tarbiat Modares University, Tehran, Iran

ABSTRACT**Article History:**

Received: 06. December. 2023

Revised: 28. February. 2024

Accepted: 03. March. 2024

Available online: 12. May. 2024

Keywords: Proportional Navigation, Guidance, Miss Distance Analysis, Optimum Parameters, Seeker Noise.

A complete miss distance analysis of true proportional navigation is carried out due to initial heading error, step target maneuver, and seeker noise sources assuming a first-order control system using forward and adjoint methods. For this purpose, linearized equations are utilized for deterministic and stochastic analyses. Worst case analysis shows that the maximum value of the final time-miss distance plots reduces by increasing the value of the effective navigation ratio due to initial heading error and step target acceleration. The number of peaks of these curves obeys the relation of the effective navigation ratio minus 1 (or 2) due to heading error (or step target maneuver). Moreover, the normalized miss coefficients due to seeker noise sources and miss due to random target maneuver are computed and approximate formulas are presented using the curve fitting method. This leads to an approximate formula for miss distance budget. Therefore, optimum values of the effective navigation ratio and control system time constant are obtained. Finally, the preferred values of these parameters are calculated for increased RMS miss of 5%, 10%, and 20% compared to its minimum value for two scenarios.

DOI<https://doi.org/10.22034/jast.2024.428886.1170>**Introduction**

Proportional navigation (PN) is a well-known two-point guidance law. This type of guidance law and its variants have been widely used. The performance of PN is also utilized as a bench mark to their modifications and other two-point guidance laws. Therefore, a complete performance analysis of PN is needed for different circumstances. For this purpose, many works have been performed including acceleration demanding and evaluating the effect of system time constant, system order, system delay, acceleration limit, seeker noise sources, radome error slope,

nonminimum phase dynamics, and different types of target maneuvers on miss distance [1-7].

There are several tools for performance analysis of guidance laws, mainly forward and adjoint methods [8-13]. Unfortunately, the adjoint method is restricted to linear systems. In the case that the governing equations of system are normalized, the results are more suitable and the number of parameters are reduced, so the analysis is more suitable and give insight to the problem. The normalized analysis and results can be utilized to obtain approximate formulas for the problem; for example, steady-state miss coefficients due to seeker noise sources, the effect of the guidance and control system delay, and acceleration limit. These

¹ (Corresponding Author), S.H. Jalali-Naini, Associate Professor Email:shjalalinaini@modares.ac.ir

formulas are as importance as the analytical solutions and significant from the practical point of view.

The noise-induced miss distance analytical solution of True PN (TPN) is available in literature only for a first-order control system. Miss distance formulas of PN are available for the first-order control system when the effective navigation ratios are integer [8,14]. For non-integer effective navigation ratios, a formula was obtained using series solution whereas the number of series terms is finite for integer effective navigation ratios [15].

The assessment and analytical formulas were also presented for linear quadratic Gaussian (LQG) optimal guidance laws. Analytical formulas of bounds (the greatest lower bound) on the achievable RMS miss were derived for step-, exponential-, and sinusoidal target maneuvers in the presence of glint noise [16,17]. The results were extended for discrete LQG problem [18], and multiple-model-based terminal guidance laws [19].

In this study, the analysis on miss distance peaks with respect to effective navigation ratio, the relation between the number of miss distance peaks and effective navigation ratio, and RMS miss due to initial heading error and step target maneuver is presented. The RMS miss formulas are also obtained for integer effective navigation ratios ≤ 8 . Moreover, the miss distance budget formula is obtained by using approximate formulas via curve fitting, and an explicit formula is derived for the optimum effective navigation ratio. Finally, explicit formulas are obtained for the optimum effective navigation ratio and system time constant when the glint is the dominant noise source.

Linearized Single-Lag PN Guidance

The commanded acceleration of TPN is given by:

$$n_c = N'v_c\dot{\lambda} \quad (1)$$

where N' is the effective navigation ratio, v_c is the interceptor-target closing velocity, and $\dot{\lambda}$ is the line-of-sight (LOS) rate.

The block diagram of TPN is shown in Fig. 1 for a first-order control system, based on linearized

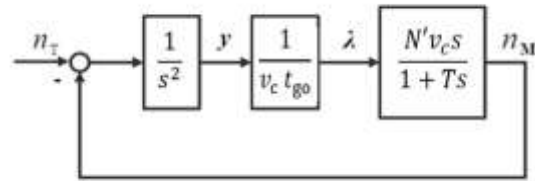


Figure 1. Block diagram of the linearized single-lag PN guidance

equations in which s is the Laplace domain variable. The linearized equations of the guidance problem are written in normalized form as follows:

$$\hat{y}' = \hat{v} \quad (2)$$

$$\hat{v}' = \hat{n}_T - \hat{n}_M \quad (3)$$

$$\hat{n}'_M = (\hat{n}_c - \hat{n}_M), \quad \hat{n}_c = N'\hat{\lambda}' \quad (4)$$

where $(\cdot)'$ is the derivative with respect to normalized time $\tau = t/T$ and

$$\hat{y} = \frac{y}{AT^2}, \quad \hat{v} = \frac{v}{AT}, \quad \hat{n}_M = \frac{n_M}{A} \\ \hat{n}_T = \frac{n_T}{A}, \quad \hat{\lambda} = \frac{v_c\lambda}{AT}, \quad \hat{\lambda}' = \frac{v_c\dot{\lambda}}{A} \quad (5)$$

in which A is the normalizing parameter (in m/s^2), λ is the LOS angle, y is the interceptor-target separation along the direction perpendicular to the initial LOS in the linearized geometry ($\dot{y} = n_T - n_M$), n_T is the target acceleration, and n_M is the achieved commanded acceleration, both of them are assumed to be in the direction perpendicular to the initial LOS. By using the small angle approximation, we have $\lambda = y/v_c t_{go}$ where $t_{go} = t_f - t$ is the time-to-go until intercept. The closing velocity is also assumed to be constant. Fortunately, the closing velocity is omitted from the equations. Normalized miss distance can then be approximated by $\hat{y}(\tau_f)$ in which $\tau_f = t_f/T$.

The equations are normalized to reduce the number of parameters. Therefore, the normalized miss becomes a function of the effective navigation ratio and normalized final time t_f/T . The analysis is performed for two cases:

- a) $n_T = 0$ & Heading Error $\neq 0$,
- b) $n_T \neq 0$ & Heading Error = 0.

The normalizing parameter is chosen $A = v_0$ for the first case whereas it is set to n_T for the second one.

$$v_0 = -v_M \sin(HE), \quad \hat{v}_0 = -1 \quad (6)$$

where v_M is the interceptor velocity. The preceding relation is valid for head on or tail chase

engagement. In the case of linearization about the collision course, the simplified relation is $\nu_o = -\nu_M \text{HE}$ using the small angle assumption.

Analytical Solutions

An analytical solution of miss due to heading error is available for an integer N' using the inverse Laplace transform of the following formula [8]:

$$\frac{\text{MD}}{-\nu_M \text{HE}}(s) = \frac{1}{s^2} \left[s / \left(s + \frac{1}{T} \right) \right]^{N'} \quad (7)$$

Also, the series form solution is given by [4]

$$\frac{\text{MD}}{-T \nu_M \text{HE}} = -e^{-x} \sum_{j=1}^{N'-1} \frac{(N'-2)! (-x)^j}{(j-1)! (N'-j-1)! j!} \quad (8)$$

where $x = t_f/T$. Note that the denominator of the preceding relations is $T\nu_o$ (see Eq. 6). The sinus function may be simplified to its argument based on the small angle approximation.

Miss due to step target maneuver is given by [8]

$$\frac{\text{MD}}{n_T}(s) = \frac{1}{s^3} \left[s / \left(s + \frac{1}{T} \right) \right]^{N'} \quad (9)$$

The inverse Laplace transform is simply available for an integer effective navigation ratio. The series form solution is also given by [14]

$$\frac{\text{MD}}{n_T T^2} = e^{-x} \sum_{j=2}^{N'-1} \frac{(N'-3)! (-x)^j}{(j-2)! (N'-j-1)! j!} \quad (10)$$

The preceding series solutions for $N' = 2, 3, 4, \dots, 8$ can be viewed in Appendix A for the two mentioned cases.

Since the normalized miss is a function of two parameters N' and t_f/T , and miss distance varies about the t_f -axis for practical values of N' and $t_f < 12T$, a useful parameter is the root mean square (or mean of the absolute) value of the miss between two specified final times, that is, for the interval $[t_{f1} \ t_{f2}]$:

$$\text{RMS MD} = \sqrt{\frac{1}{t_{f2} - t_{f1}} \int_{t_{f1}}^{t_{f2}} \text{MD}^2(t_f) dt_f} \quad (11)$$

$$\text{Mean } |\text{MD}| = \frac{1}{t_{f2} - t_{f1}} \int_{t_{f1}}^{t_{f2}} |\text{MD}(t_f)| dt_f \quad (12)$$

In our analysis, we set $t_{f1} = 0$ and $t_{f2} = t_f$; however, we have kept the notation t_{f2} in the figures to avoid ambiguity. Therefore, the RMS miss becomes only a function of N' , which helps us to determine an optimum value or a preferred range for N' .

The RMS miss formulas can be obtained analytically for integer values of N' . For example, the RMS miss due to heading error for $N' = 2$ is given by

$$\left. \frac{2 \text{RMS MD}}{T \nu_M |\text{HE}|} \right|_{N'=2} = \sqrt{\frac{1 - e^{-2x}(2x^2 + 2x + 1)}{x}} \quad (13)$$

In a similar way, the RMS miss distance due to step target maneuver is obtained for $N' = 3$ as follows:

$$\left. \frac{4 \text{RMS MD}}{T^2 n_T} \right|_{N'=3} = \sqrt{\frac{3 - e^{-2x}(2x^4 + 4x^3 + 6x^2 + 6x + 3)}{x}} \quad (14)$$

By applying the rules of the adjoint method from Ref. [8], the adjoint model of the block diagram of Fig. 1 is plotted in Fig. 2. Mean absolute and RMS values of miss have been added to the adjoint block diagram for $t_{f1} = 0$ and $t_{f2} = t_f$. The miss distance results for non-integer N' are obtained numerically using forward and adjoint models.

It is worth noting that the above-mentioned RMS miss due to step target maneuver is equivalent to the problem that a target has a step maneuver (either plus or minus n_T) with uniformly distributed starting time over the final time t_f .

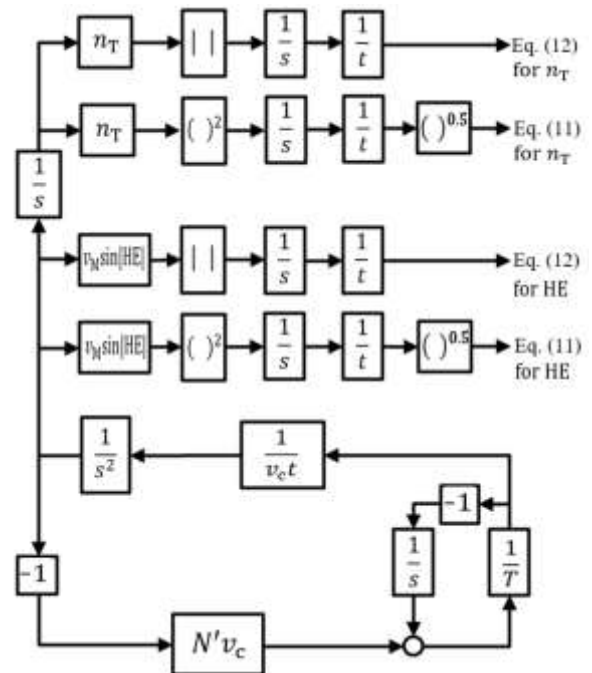


Figure 2. Block diagram of the adjoint model of the linearized TPN ($t_{f1} = 0$ & $t_{f2} = t_f$ in Eqs. 11 & 12)

MD Analysis due to Heading Error

First, normalized miss distance analysis due to heading error is performed using forward and adjoint methods (case a: $HE \neq 0, n_T = 0$). For this purpose, the absolute value of the miss distance versus the final time and effective navigation ratio is shown in Fig. 3. This result is also plotted in two dimension in Fig. 4 for different values of effective navigation ratios. As seen in the figures, increasing the effective navigation ratio decreases the value of the first peak (from the left) of the t_f -|MD| plot. The behavior of the second peak versus N' is different. Increasing N' increases the value of the second peak for $2 \leq N' < 4.32$ then decreases for $N' > 4.32$. To investigate this behavior more accurately, the value of the i th peak, $|MD_{Pi}|$, versus the effective navigation ratio is depicted in Fig. 5 for $i=1,2,3,4,5$. The important result is that the worst miss value decreases by increasing the effective navigation ratio (checked for ≤ 25). This behavior is not seen for a fifth-order binomial control system which has an optimum value of $N' = 3.75$ based on the worst case analysis. Now the question is what the number of peaks (n_p) is for the t_f -|MD| plot. For the integer value of N' we have found the relation $n_p=N'-1$ (checked for $N' \leq 25$ from MD formulas as presented in Appendix A). The number of peaks are obtained numerically by trial and error, plotted in Fig. 6 for integer and non-integer values of N' (peak values greater than 0.0005 is considered). The results are in close agreement for integer values according to the relation $n_p=N'-1$, shown by star in Fig. 6.

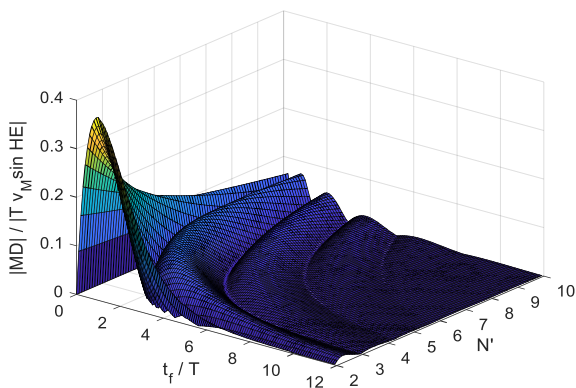


Figure 3. Absolute miss due to heading error versus final time and N' in normalized form.

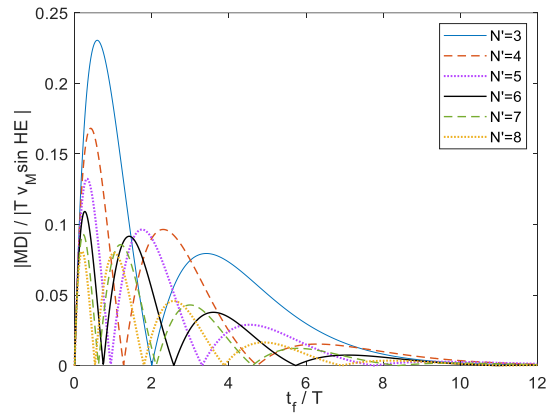


Figure 4. Absolute value of miss distance due to heading error in normalized form.

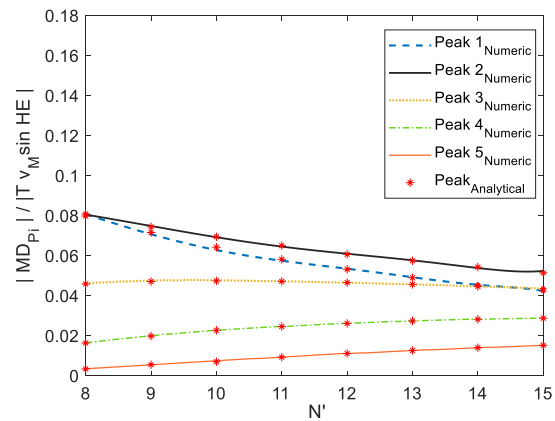
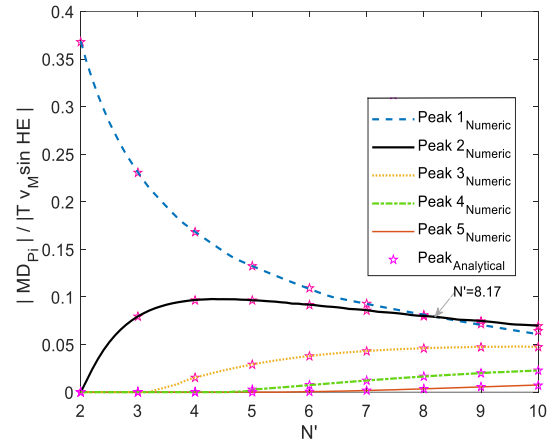


Figure 5. Normalized absolute miss for the i th peak of t_f -|MD| plot due to heading error ($k=1,2,3,4,5$).

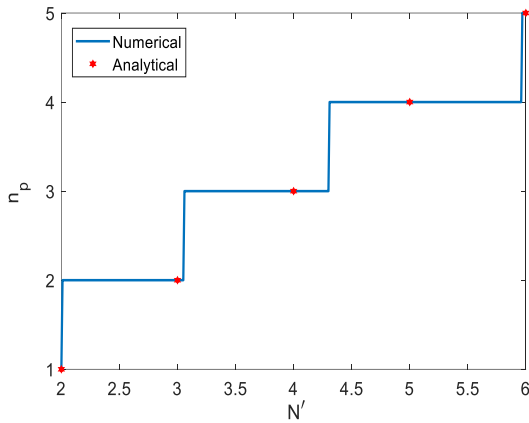


Figure 6. Number of peaks of t_f -|MD| plot due to heading error.

Figure 7 shows the RMS miss due to initial heading error over the interval $[0, t_{f2}]$ versus N' and t_{f2} in normalized form. The results are also plotted in two-dimension for various values of N' in Fig. 8. Moreover, the mean absolute miss versus t_{f2} is depicted in Fig. 9. From the figures, it seems the RMS (or the mean absolute) value decreases by increasing N' for a specified value of t_{f2} . This can be seen more clearly in Fig. 10 that shows the RMS miss versus N' for different values of $t_{f2} = T, 2T, 4T, 6T, 8T, 10T, 12T$ (i.e., the interval length $t_{f2} - t_{f1}$; $t_{f1} = 0$).

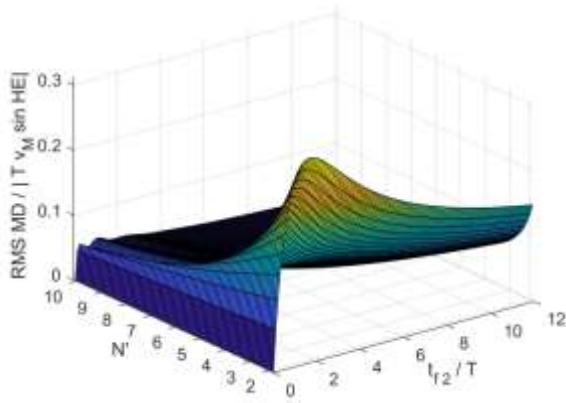


Figure 7. RMS miss in the interval $[0, t_{f2}]$ versus t_{f2} and N' in normalized form (due to HE).

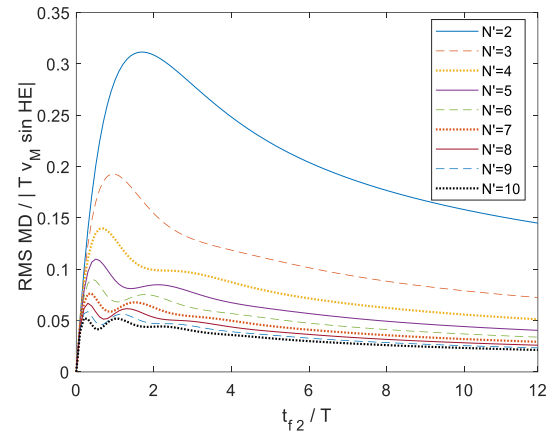


Figure 8. RMS miss in the interval $[0, t_{f2}]$ versus t_{f2} in normalized form (due to HE).

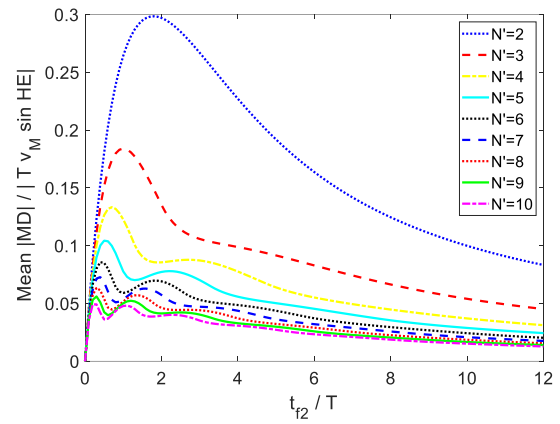


Figure 9. Mean absolute miss in the interval $[0, t_{f2}]$ versus t_{f2} in normalized form for different values of the effective navigation ratio (due to HE)

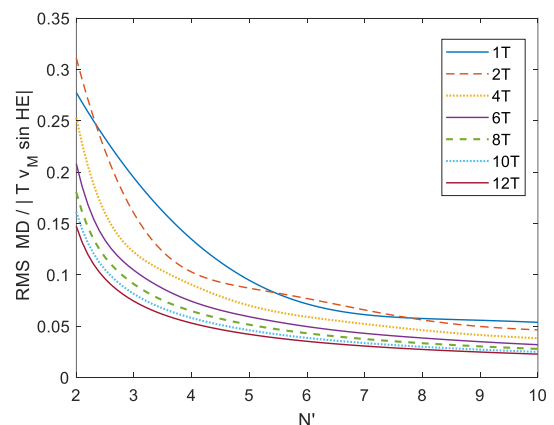


Figure 10. RMS miss in the interval $[0, t_{f2}]$ versus N' for $t_{f2}/T=1,2,4,6,8,10,12$ in normalized form (due to HE)

MD Analysis due to Step Target Maneuver

In the second step, miss distance analysis is carried out for a target with a constant acceleration in

normalized form (case b: $HE = 0, n_T \neq 0$). The results are obtained by two methods: the forward and adjoint methods. The analysis is performed the same as the previous section. Normalized miss distance curves are plotted in Figs. 11 and 12. The behavior of the t_f -|MD| peaks is shown in Fig. 13. For this case, the number of peaks obeys the relation $n_p = N' - 2$ (checked for $N' \leq 25$) according to Fig. 14 for integer values of N' . Normalized peak values greater than 0.001 is considered in Fig. 14 for non-integer values of N' . As shown in the figures, miss distance is reduced by increasing the effective navigation ratio for the worst case (checked for $N' \leq 20$).

As an important behavior, the miss distance in the t_f -|MD| curves becomes zero due to HE at a

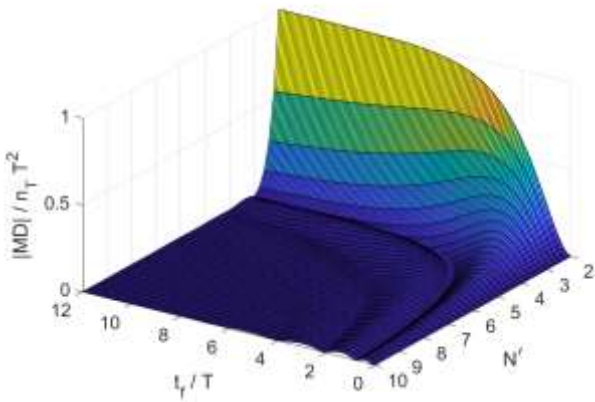


Figure 11. Absolute miss distance due to step target maneuver versus final time and N' in normalized form ($n_T > 0$).

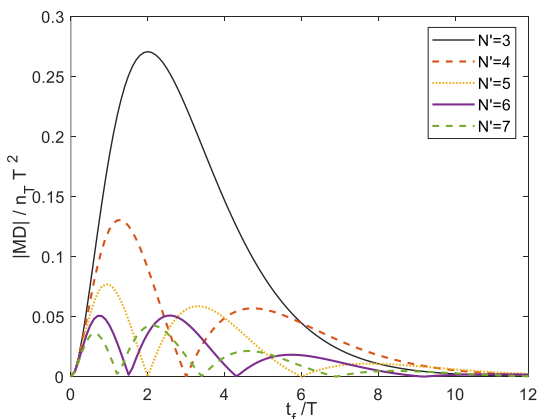


Figure 12. Absolute miss distance due to step target maneuver in normalized form ($n_T > 0$).

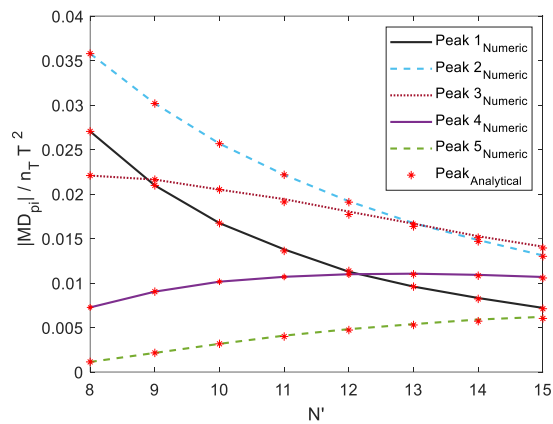
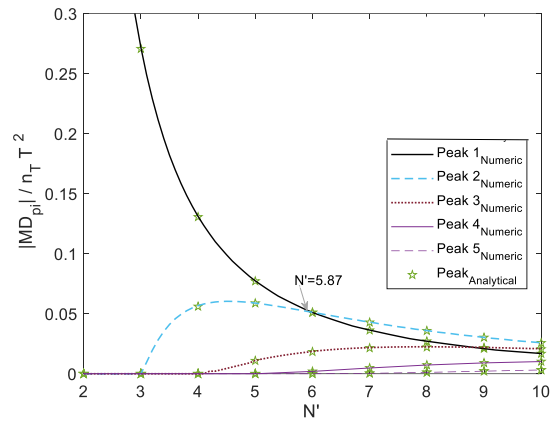


Figure 13. Normalized miss distance for the k th peak of the t_f -|MD| plot due to step target maneuver ($k=1,2,3,4,5, n_T > 0$).

specified final time (or several final times, depending of the value of N'), whereas its absolute miss value due to step target maneuver has a local

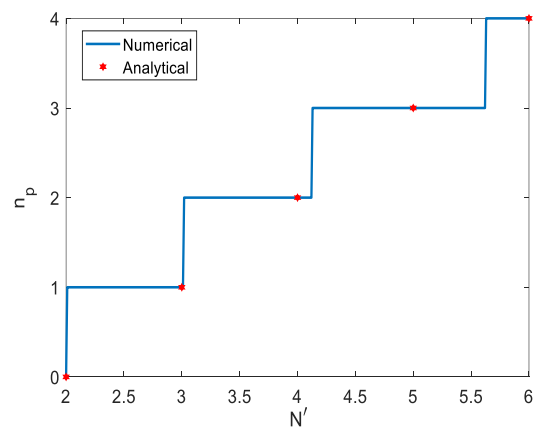


Figure 14. Number of peaks of the t_f -|MD| plot due to step target maneuver.

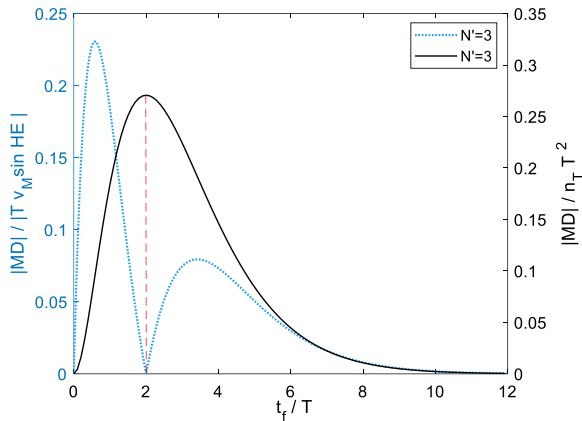


Figure 15. Opposite behavior of miss due to HE against miss due to step maneuver for $t_f/T=2$ ($N' = 3$)

maximum at the same final time. Hence, we see the miss distance has an opposite behavior with respect to the final time for the two cases a and b as seen in Fig. 15. As a result, a modification on the effective navigation ratio based on HE may not work against a step target maneuver and vice versa, as seen in Ref [20] in which a modified profile for N' based on HE, did not work against a step target maneuver when N' was chosen as a function of the angle between the relative velocity and LOS. Therefore, N' was designed as a function of this angle and its rate.

The RMS MD analysis is shown in Figs. 16, 17, and 19. As mentioned before, these results are the same as the ones for the stochastic case when the starting time of a step maneuver is uniformly distributed over the final time. The mean absolute miss is also plotted in Fig. 18.

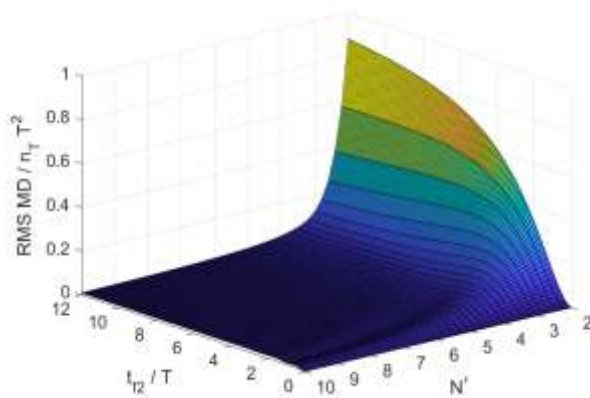


Figure 16. RMS miss distance in the interval $[0 t_{f2}]$ versus t_{f2} and N' in normalized form due to a step target maneuver ($n_T > 0$).

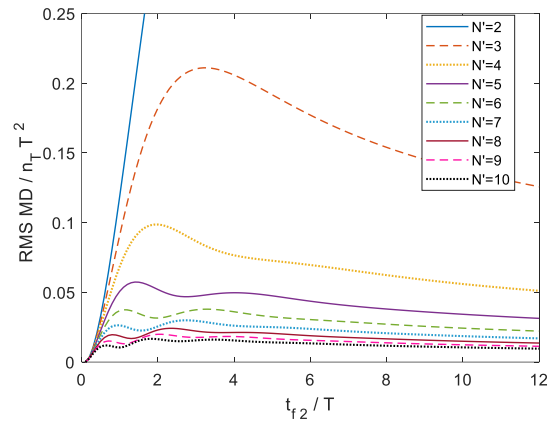


Figure 17. RMS miss distance in the interval $[0 t_{f2}]$ versus t_{f2} in normalized form for different values of the effective Navigation ratios (due to n_T).

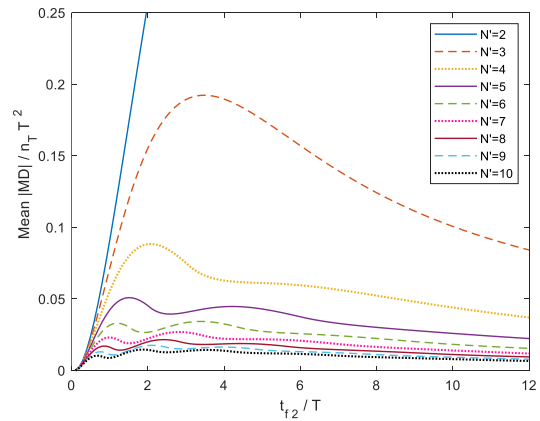


Figure 18. Mean absolute miss in the interval $[0 t_{f2}]$ versus t_{f2} in normalized form for different values of the effective Navigation ratios (due to $n_T > 0$).

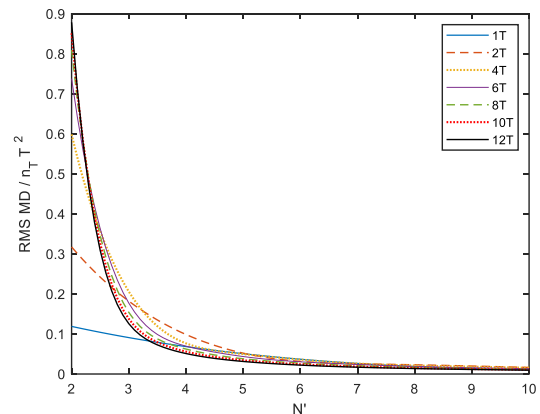


Figure 19. RMS miss in the interval $[0 t_{f2}]$ versus N' for different values of $t_{f2}/T=1,2,4,6,8,10,12$ in normalized form (due to n_T).

MD Analysis due to Seeker Noise

In the third step, the normalized miss coefficients due to seeker noise sources are obtained using adjoint model according to Ref. [8]. The normalized miss coefficient due to glint noise (k_{GL}) versus the effective navigation ratio is depicted in Fig. 20. A linear relation is also obtained for k_{GL}^2 as follows:

$$k_{GL}^2(N') = 0.864 N' - 0.541 \quad (15)$$

Using the preceding relation, the maximum absolute error of k_{GL} is 0.004 for $3 \leq N' \leq 6$. The maximum absolute error increases to 0.03 for $2 \leq N' < 8$.

The normalized miss coefficient due to range-independent noise (k_{FN}) versus the effective navigation ratio is plotted in Fig. 21. For this case, the following curve fitting is obtained:

$$k_{FN}^2(N') = 0.0295 N' + 0.194 \quad (16)$$

with the maximum absolute error of 0.001 in k_{FN} for $3 \leq N' \leq 6$. The maximum absolute error increases to 0.0075 for $2 \leq N' < 8$.

Figure 22 shows the normalized miss coefficient due to semi-active range dependent noise (k_{RN}) versus the effective navigation ratio. The following equation has a maximum absolute error of 0.0027 in k_{RN} when $3 \leq N' \leq 7$:

$$k_{RN}^2(N') = 0.099 N' + 0.826 \quad (17)$$

The value of maximum absolute error is increased to 0.05 when $2 \leq N' \leq 8$.

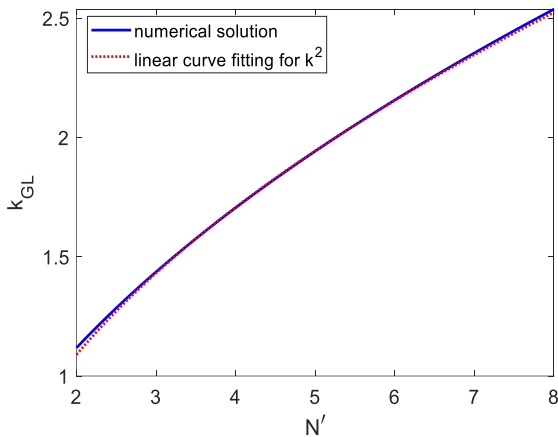


Figure 20. Steady-state glint noise coefficient and its curve fitting versus the effective navigation ratio.

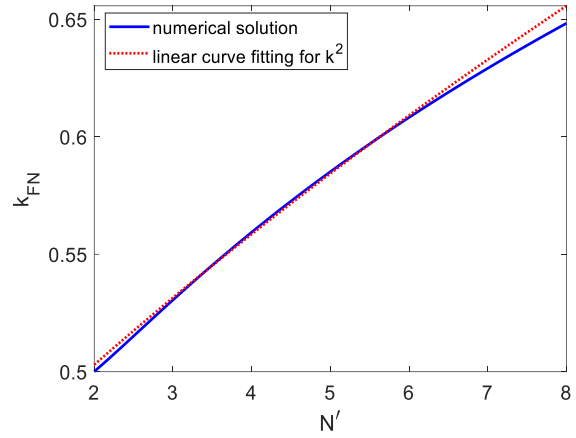


Figure 21. Steady-state range independent noise coefficient and its curve fitting versus the effective navigation ratio.

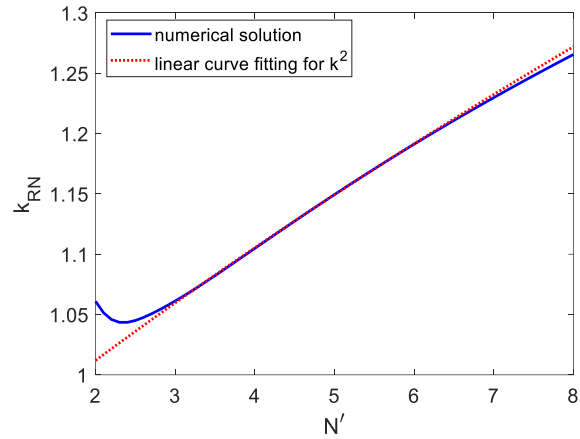


Figure 22. Steady-state semi-active range dependent noise coefficient and its curve fitting versus the effective navigation ratio.

Results and Discussion

In the previous sections, the miss distance analysis is carried out due to initial HE, step target maneuver (with the two interpretations), and seeker noise sources for semi-active radar homing interceptors. We are now to obtain the optimum value of the effective navigation ratio that minimizes the total standard deviation of miss distance. For this purpose, the step target maneuver (either plus or minus n_T) with a random starting time over the flight time and seeker noise sources are considered. The total standard deviation is given by

$$\sigma^2 = \sigma_{n_T}^2 + \sigma_{GL}^2 + \sigma_{FN}^2 + \sigma_{RN}^2 \quad (18)$$

where each subscript corresponds to a seeker noise source, similar to the normalized miss coefficients

due to seeker noise sources, except the first one in the right hand side that stands for a random target maneuver. Substituting the relations for the normalized miss coefficients due to seeker noise sources, we have

$$\sigma^2(N', T) = \sigma_{n_T}^2(N', T) + \frac{1}{T} k_{GL}^2(N') \phi_{GL} + k_{FN}^2(N') \phi_{FN} T v_c^2 + \frac{1}{R_A^2} k_{RN}^2(N') \phi_{RN} T^3 v_c^4 \quad (19)$$

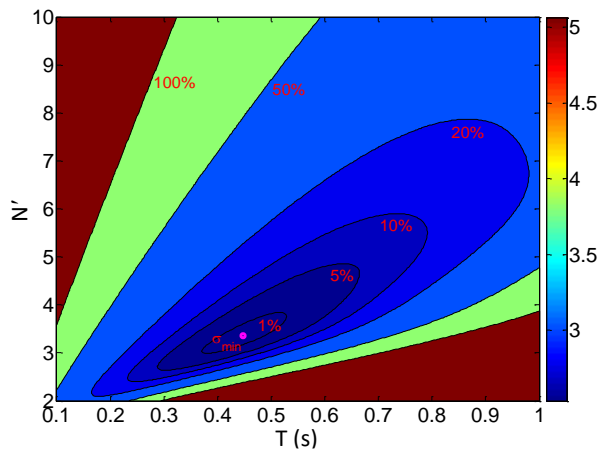
where ϕ 's are the power spectral densities of the seeker noise sources according to the model of Ref. [8], with the subscripts defined as in σ 's. The power spectral density of a range dependent noise is defined at a reference range R_A [8].

First, the optimization may be carried out numerically using Eq. (19) when T is also considered as a design variable. The results are shown in Figs. 23 and 24 for two scenarios as follows:

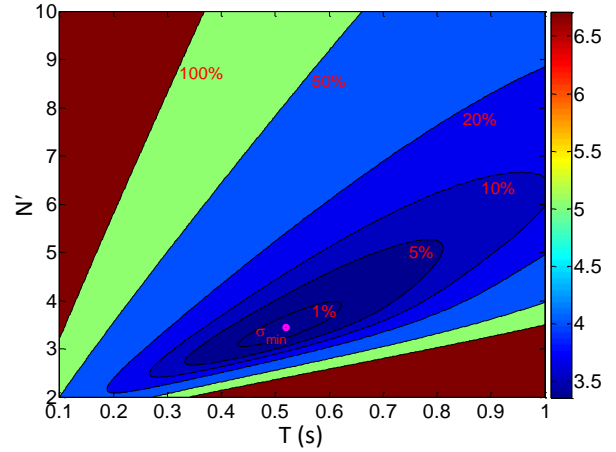
Scenario 1: $n_T = 6g \text{ m/s}^2$, $\phi_{GL} = 1 \text{ m}^2/\text{Hz}$, $\phi_{FN} = 2 \times 10^{-8} \text{ rad}^2/\text{Hz}$, $\phi_{RN} = 8 \times 10^{-6} \text{ rad}^2/\text{Hz}$, $v_c = 1500 \text{ m/s}$, $R_A = 6000 \text{ m}$;

Scenario 2: $n_T = 6g \text{ m/s}^2$, $\phi_{GL} = 2 \text{ m}^2/\text{Hz}$, $\phi_{FN} = 2 \times 10^{-8} \text{ rad}^2/\text{Hz}$, $\phi_{RN} = 2 \times 10^{-6} \text{ rad}^2/\text{Hz}$, $v_c = 1200 \text{ m/s}$, $R_A = 3000 \text{ m}$.

As seen in Fig. 23 b, the optimum values are $N'^* = 3.42$ and $T^* = 0.52$ when $t_f = 5 \text{ s}$ for Scenario 2. The benefit of the analysis is that the desired values of N' and T under a specific increased amount in RMS MD (in percent) are also obtained and plotted in Fig. 23 ($t_f = 5 \text{ s}$). Figure 24 shows the optimum values of N' and T versus the final time for the two scenarios using the grid search method.



a) Scenario 1



b) Scenario 2

Figure 23. Optimum values for N' and T , and their values for 1,5,10,20,50,100% increased RMS miss with respect to σ_{\min} ($t_f = 5 \text{ s}$)

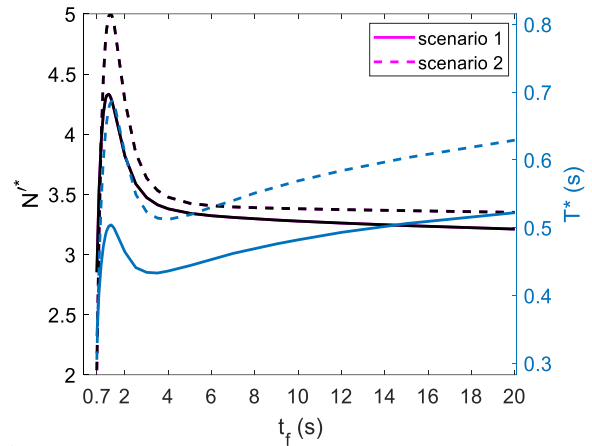


Figure 24. Comparison of N'^* and T^* for the two scenarios

To go further analytically, a relation for the case of maneuvering target with uniformly distributed starting time is obtained using curve fitting, that is ($N' \geq 2.6$),

$$\hat{\sigma}_{n_T}^2(N', x) = \frac{\sigma_{n_T}^2}{(n_T T^2)^2} = \frac{0.085}{x (N' - 2.32)^2} \quad (20)$$

where $x = t_f/T$ as mentioned before. The accuracy of the preceding relation is shown in Fig. 25 for different values of $N' \geq 2.8$. By substitution of the obtained approximate relations in Eq. (19), we have

$$\sigma^2(N', T) = \frac{0.085 n_T^2 T^5}{t_f (N' - 2.32)^2} + \frac{1}{T} (0.864 N' - 0.541) \phi_{GL} + (0.0295 N' + 0.194) \phi_{FN} T v_c^2 + \frac{1}{R_A^2} (0.099 N' + 0.826) \phi_{RN} T^3 v_c^4 \quad (21)$$

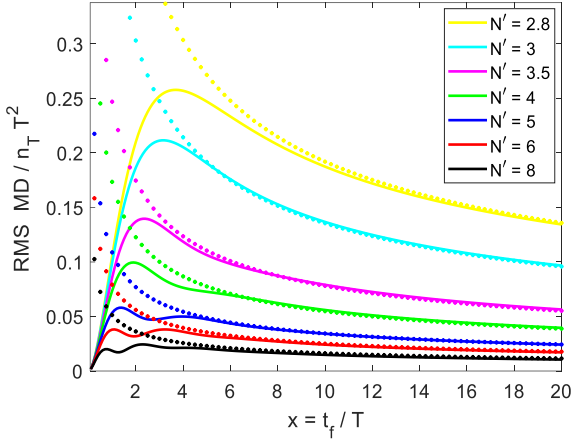


Figure 25. RMS miss distance due to random target maneuver versus flight time in normalized form (solid lines: numerical solution; dotted lines: curve fitting)

When the design variable is only the effective navigation ratio, the optimum N' is derived as follows:

$$\frac{\partial \sigma^2}{\partial N'} = \frac{\partial \sigma_{nT}^2}{\partial N'} + \frac{\partial \sigma_{GL}^2}{\partial N'} + \frac{\partial \sigma_{FN}^2}{\partial N'} + \frac{\partial \sigma_{RN}^2}{\partial N'} \quad (22)$$

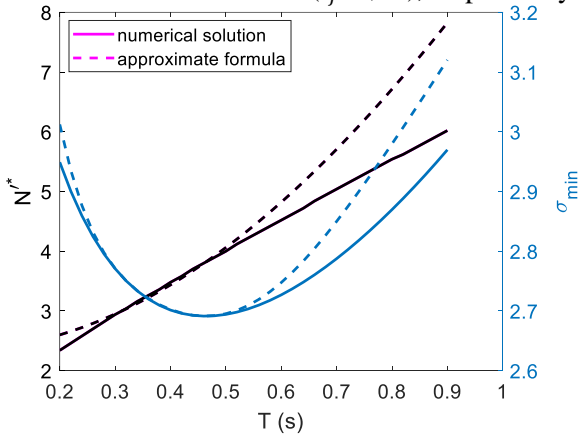
$$\frac{\partial \sigma^2}{\partial N'} = \frac{-0.17}{t_f(N' - 2.32)^3} n_T^2 T^5 + \frac{0.864}{T} \phi_{GL} + 0.0295 \phi_{FN} T v_c^2 + \frac{0.099}{R_A^2} \phi_{RN} T^3 v_c^4 \quad (23)$$

Hence, the optimum value is given by

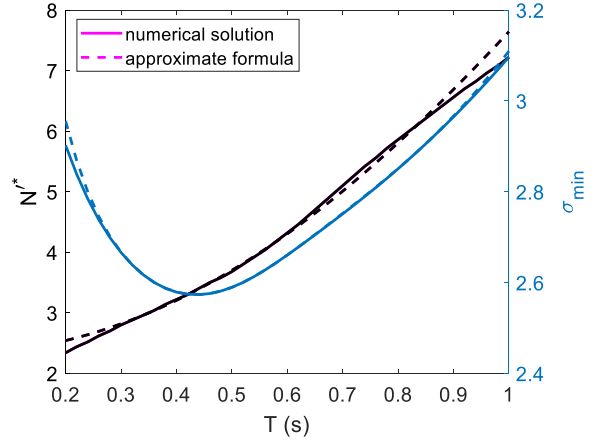
$$N' = 2.32 +$$

$$\sqrt[3]{\frac{17 n_T^2 T^6 / t_f}{86.4 \phi_{GL} + 2.95 \phi_{FN} T^2 v_c^2 + \frac{9.9}{R_A^2} \phi_{RN} T^4 v_c^4}} \quad (24)$$

The optimum value of N' , according to the preceding relation, is plotted in Figs. 26 and 27 for Scenario 1 and Scenario 2 ($t_f=2,4$ s), respectively.



a) $t_f = 2$ (s)



b) $t_f = 4$ (s)

Figure 26. Comparison of numerical solution with approximate formula for N'^* and σ_{min} versus T for Scenario 1

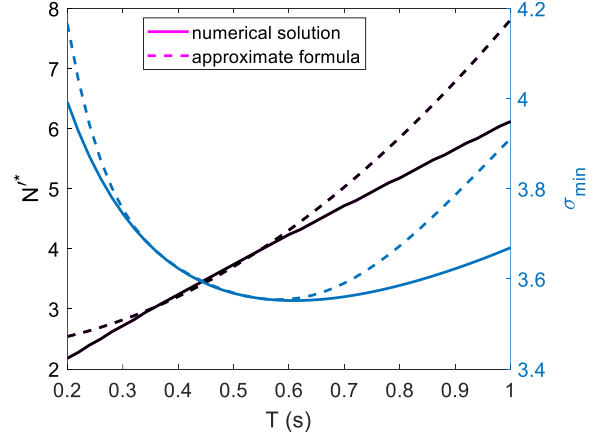
Its associated standard deviation is calculated from Eq. (21). These results are compared to the exact solution, obtained numerically. As seen in these figures, the accuracy of the approximate formula is decent for $t_f=4$ s when $0.3 < T < 0.9$; however, it is case dependent. For $t_f=2$ s, the approximate formula is still good for optimization with two variables (N' , T). For this case, the following relation is also needed:

$$\frac{\partial \sigma^2}{\partial T} = \frac{\partial \sigma_{nT}^2}{\partial T} + \frac{\partial \sigma_{GL}^2}{\partial T} + \frac{\partial \sigma_{FN}^2}{\partial T} + \frac{\partial \sigma_{RN}^2}{\partial T} \quad (25)$$

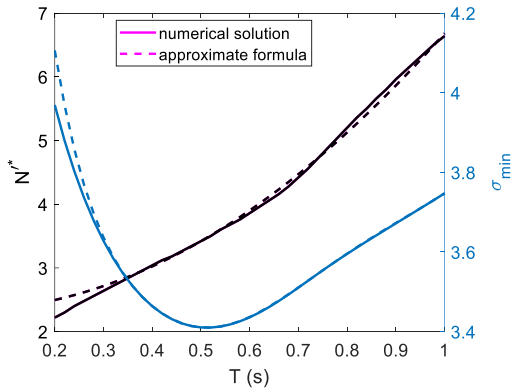
Substitution yields,

$$\frac{\partial \sigma^2}{\partial T} = \frac{5(0.085)n_T^2 T^4}{t_f(N' - 2.32)^2} - \frac{1}{T^2} (0.864 N' - 0.541)\phi_{GL} + (0.0295 N' + 0.194)\phi_{FN} v_c^2 + \frac{3}{R_A^2} (0.099 N' + 0.826)\phi_{RN} T^2 v_c^4 \quad (26)$$

The preceding relation is set to zero, and then the



a) $t_f = 2$ (s)



b) $t_f = 4$ (s)

Figure 27. Comparison of approximate formula with numerical solution for N^* and σ_{\min} versus T for Scenario 2

effective navigation ratio in Eq. (26) is replaced by Eq. (24) resulting in a transcendental equation in terms of T^* . Another way is to solve Eq. (21) for a range of values of T after replacing N' by Eq. (24), so the minimum value can be determined numerically. As an advantage of the second way, this range of values of T begins with the minimum possible value of system time constant.

The accuracy of the approximate formula is more investigated and the results are compared in Table 1 with the exact solution, obtained numerically. The approximate formula gives a good results for $t_f > 4$ s both in N^* and T^* ; however, the results are also acceptable for $t_f \geq 1$ because the values of standard deviation of the both methods are very close, as seen in Table 1.

Table 1. Accuracy of the approximate formulas (24) and (26) for Scenario 2

| t_f (s) | Numerical Solution | | | Approximate Formulas | | |
|-----------|--------------------|-----------|---------------------|----------------------|-------|-----------------|
| | N^* | T^* (s) | σ_{\min} (m) | N^* | T^* | σ_{\min} |
| 1 | 4.482 | 0.601 | 3.7075 | 3.432 | 0.399 | 3.7532 |
| 1.5 | 4.925 | 0.686 | 3.6154 | 3.426 | 0.426 | 3.6758 |
| 2 | 4.284 | 0.610 | 3.5512 | 3.422 | 0.446 | 3.5938 |
| 2.5 | 3.849 | 0.550 | 3.5106 | 3.418 | 0.462 | 3.5304 |
| 3 | 3.643 | 0.524 | 3.4745 | 3.414 | 0.475 | 3.4824 |
| 3.5 | 3.539 | 0.515 | 3.4406 | 3.411 | 0.487 | 3.4436 |
| 4 | 3.484 | 0.514 | 3.4091 | 3.407 | 0.497 | 3.4102 |
| 4.5 | 3.453 | 0.516 | 3.3801 | 3.404 | 0.506 | 3.3805 |
| 5 | 3.431 | 0.521 | 3.3535 | 3.401 | 0.515 | 3.3537 |
| 6 | 3.414 | 0.531 | 3.3068 | 3.396 | 0.529 | 3.3069 |
| 7 | 3.405 | 0.542 | 3.2671 | 3.391 | 0.542 | 3.2672 |
| 8 | 3.398 | 0.553 | 3.2329 | 3.386 | 0.553 | 3.2330 |
| 9 | 3.394 | 0.562 | 3.2029 | 3.381 | 0.562 | 3.2030 |
| 10 | 3.39 | 0.571 | 3.1763 | 3.377 | 0.571 | 3.1764 |
| 12 | 3.382 | 0.586 | 3.1308 | 3.369 | 0.587 | 3.1309 |
| 15 | 3.372 | 0.605 | 3.0761 | 3.358 | 0.606 | 3.0763 |
| 20 | 3.357 | 0.631 | 3.0075 | 3.343 | 0.631 | 3.0076 |
| 30 | 3.332 | 0.667 | 2.9144 | 3.317 | 0.667 | 2.9146 |
| 50 | 3.294 | 0.712 | 2.8034 | 3.279 | 0.712 | 2.8036 |
| 100 | 3.230 | 0.773 | 2.6644 | 3.215 | 0.773 | 2.6645 |

Approximate Formula for T^*

Since the glint noise is the dominant noise source, an explicit approximate formula for the optimum time constant can be obtained as follows:

$$T^{*2} = \frac{(c_1 N_0 + c_0)}{3 c_T^{1/3}} \left(\frac{2}{c_1}\right)^{2/3} \left(\frac{t_f \phi_{GL}}{n_T^2}\right)^{1/3} \quad (27)$$

$$N^* = \frac{5}{3} N_0 + \frac{2 c_0}{3 c_1} \quad (28)$$

where c_0 , c_1 , N_0 , and c_T are constants and defined as follows:

$$k_{GL}^2(N') = c_1 N' + c_0 \quad (29)$$

$$\hat{\sigma}_{n_T}^2(N', x) = \frac{\sigma_{n_T}^2}{(n_T T^2)^2} = \frac{c_T}{x (N' - N_0)^2} \quad (30)$$

For this case, the optimum value of N' has been obtained as a constant according to Eq. (28) using the equations obtained by curve fitting for the glint noise and target maneuver ($\phi_{FN} = 0, \phi_{RN} = 0$).

For example, Eqs. (27) and (28) for Scenario 2 are given by ($\phi_{FN} = 0, \phi_{RN} = 0$)

$$T^{*2} = 1.9415 \left(\frac{t_f \phi_{GL}}{n_T^2}\right)^{1/3} \quad (31)$$

$$N^* = 3.449 \quad (32)$$

The obtained results for the approximate solution and the exact solution can be viewed in Table 2 for Scenario 2 when $\phi_{FN} = 0$ and $\phi_{RN} = 0$. Moreover, the optimum values and their values for 1,5,10,20,50,100% increased RMS miss with respect to σ_{\min} are seen in Fig. 28 when $t_f = 4$ s. The optimum N' is shown in Fig. 29 for a given time constant, and compared to the exact solution at $t_f = 4$ s when $\phi_{FN} = 0$ and $\phi_{RN} = 0$.

The optimum values of N' and T , obtained from Eqs. (27) and (28), are also plotted in Fig. 30 for $t_f > 1$ s, and compared to the exact solution. As seen in Fig. 30, although the accuracy of N^* and T^* are not good for $1 < t_f < 3.5$ s, but the RMS miss is within the 3% region according to Table 2 and Fig. 28.

As a modification, the optimum effective navigation ratio can be computed using Eqs. (24) and (31), that is,

$$T^{*2} = 1.9415 \left(\frac{t_f \phi_{GL}}{n_T^2}\right)^{1/3} \quad (33)$$

$$N^* = 2.32 + T^{*2} \times \quad (34)$$

$$\sqrt[3]{\frac{17 n_T^2 / t_f}{86.4\phi_{GL} + 2.95\phi_{FN} T^{*2} v_c^2 + \frac{9.9}{R_A^2} \phi_{RN} T^{*4} v_c^4}}$$

The accuracy of the preceding formulas is shown in Fig. 31 and compared with the exact solution and approximate formulas (24) and (26). The results can be viewed in Table 3 for several final times. As the results show, the modification slightly improves the results for $t_f < 5$ s. For a better accuracy, the coefficients c_T and N_0 can be determined by a lookup table.

Table 2. Accuracy of the approximate formulas (31) and (32) for Scenario 2 ($\phi_{FN} = 0, \phi_{RN} = 0$)

| t_f (s) | Numerical Solution | | | Approximate Formulas | | |
|-----------|--------------------|-----------|--------------------|----------------------|-------|----------------|
| | N^{**} | T^* (s) | σ_{min} (m) | N^{**} | T^* | σ_{min} |
| 1 | 6.872 | 0.981 | 3.6767 | 3.449 | 0.402 | 3.7466 |
| 1.5 | 6.645 | 0.995 | 3.5719 | 3.449 | 0.430 | 3.6672 |
| 2 | 4.574 | 0.670 | 3.5291 | 3.449 | 0.451 | 3.5834 |
| 2.5 | 3.943 | 0.571 | 3.4960 | 3.449 | 0.468 | 3.5191 |
| 3 | 3.697 | 0.537 | 3.4621 | 3.449 | 0.483 | 3.4708 |
| 3.5 | 3.583 | 0.525 | 3.4289 | 3.449 | 0.495 | 3.4319 |
| 4 | 3.524 | 0.523 | 3.3974 | 3.449 | 0.507 | 3.3984 |
| 4.5 | 3.493 | 0.526 | 3.3682 | 3.449 | 0.517 | 3.3685 |
| 5 | 3.475 | 0.531 | 3.3412 | 3.449 | 0.526 | 3.3413 |
| 6 | 3.461 | 0.543 | 3.2936 | 3.449 | 0.542 | 3.2936 |
| 7 | 3.458 | 0.555 | 3.2528 | 3.449 | 0.556 | 3.2529 |
| 8 | 3.458 | 0.567 | 3.2176 | 3.449 | 0.569 | 3.2177 |
| 9 | 3.459 | 0.579 | 3.1866 | 3.449 | 0.580 | 3.1867 |
| 10 | 3.460 | 0.589 | 3.1590 | 3.449 | 0.590 | 3.1592 |
| 12 | 3.463 | 0.607 | 3.1117 | 3.449 | 0.608 | 3.1119 |
| 15 | 3.466 | 0.631 | 3.0547 | 3.449 | 0.631 | 3.0549 |
| 20 | 3.468 | 0.662 | 2.9825 | 3.449 | 0.662 | 2.9827 |
| 30 | 3.471 | 0.709 | 2.8836 | 3.449 | 0.709 | 2.8838 |
| 50 | 3.473 | 0.773 | 2.7635 | 3.449 | 0.772 | 2.7637 |
| 100 | 3.476 | 0.868 | 2.6085 | 3.449 | 0.866 | 2.6087 |

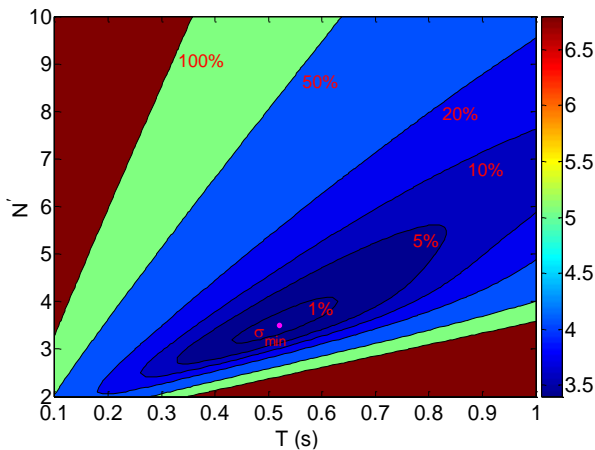


Figure 28. Optimum values for N' and T , and their values for 1, 5, 10, 20, 50% increased RMS miss w.r.t σ_{min} for Scenario 2 at $t_f = 4$ s ($\phi_{FN} = 0, \phi_{RN} = 0$)

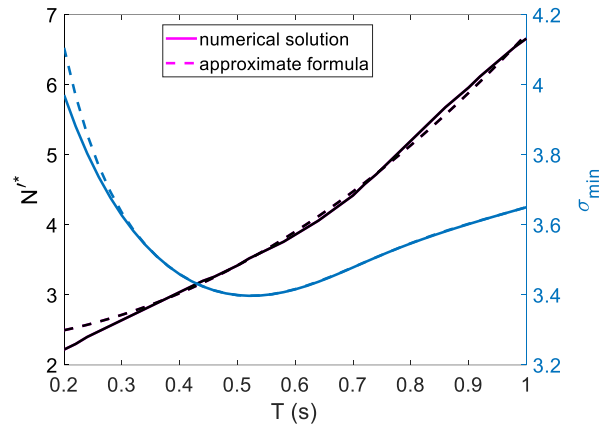


Figure 29. Comparison of approximate formula (24) with numerical solution for a given time constant when $t_f = 4$ s ($\phi_{FN} = 0, \phi_{RN} = 0$)

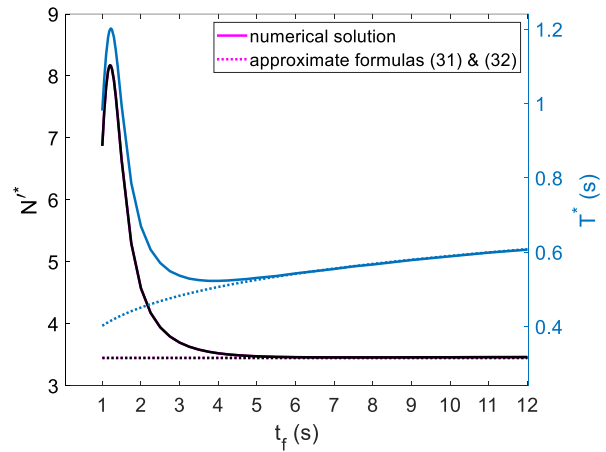
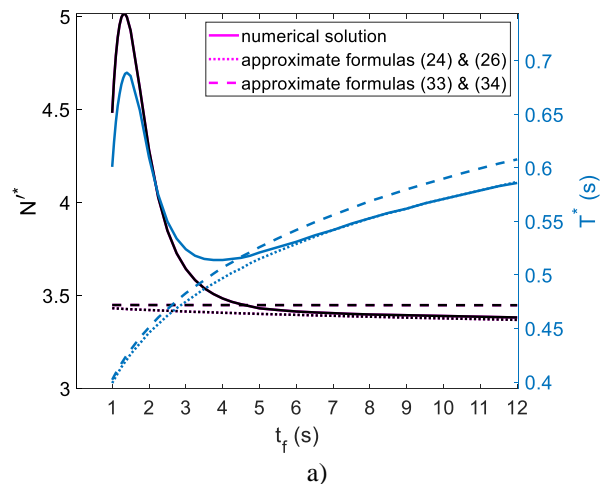


Figure 30. Comparison of approximate formulas (27) and (28) with numerical solution for Scenario 2 ($\phi_{FN} = 0, \phi_{RN} = 0$)



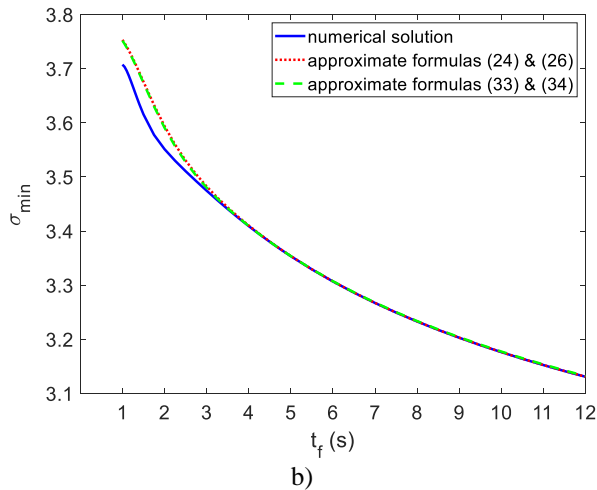


Figure 31. Comparison of approximate formulas with exact solution for scenario 2

Table 3. Accuracy of the approximate formulas (33) and (34) for Scenario 2

| t_f (s) | Numerical Solution | | | Approximate Formulas | | |
|-----------|--------------------|-----------|---------------------|----------------------|-------|-----------------|
| | N'^* | T^* (s) | σ_{\min} (m) | N'^* | T^* | σ_{\min} |
| 1 | 4.482 | 0.601 | 3.7075 | 3.4489 | 0.402 | 3.7517 |
| 1.5 | 4.925 | 0.686 | 3.6154 | 3.4489 | 0.430 | 3.6735 |
| 2 | 4.284 | 0.610 | 3.5512 | 3.4488 | 0.451 | 3.5908 |
| 2.5 | 3.849 | 0.550 | 3.5106 | 3.4487 | 0.468 | 3.5275 |
| 3 | 3.643 | 0.524 | 3.4745 | 3.4486 | 0.483 | 3.4801 |
| 3.5 | 3.539 | 0.515 | 3.4406 | 3.4486 | 0.495 | 3.4420 |
| 4 | 3.484 | 0.514 | 3.4091 | 3.4485 | 0.507 | 3.4093 |
| 4.5 | 3.453 | 0.516 | 3.3801 | 3.4485 | 0.517 | 3.3801 |
| 5 | 3.431 | 0.521 | 3.3535 | 3.4484 | 0.526 | 3.3537 |
| 6 | 3.414 | 0.531 | 3.3068 | 3.4483 | 0.542 | 3.3073 |
| 7 | 3.405 | 0.542 | 3.2671 | 3.4482 | 0.556 | 3.2678 |
| 8 | 3.398 | 0.553 | 3.2329 | 3.4481 | 0.569 | 3.2337 |
| 9 | 3.394 | 0.562 | 3.2029 | 3.4480 | 0.580 | 3.2039 |
| 10 | 3.39 | 0.571 | 3.1763 | 3.4480 | 0.590 | 3.1774 |
| 12 | 3.382 | 0.586 | 3.1308 | 3.4478 | 0.608 | 3.1321 |
| 15 | 3.372 | 0.605 | 3.0761 | 3.4476 | 0.631 | 3.0778 |
| 20 | 3.357 | 0.631 | 3.0075 | 3.4472 | 0.662 | 3.0098 |
| 30 | 3.332 | 0.667 | 2.9144 | 3.4466 | 0.709 | 2.9178 |
| 50 | 3.294 | 0.712 | 2.8034 | 3.4456 | 0.772 | 2.8093 |
| 100 | 3.230 | 0.773 | 2.6644 | 3.4436 | 0.866 | 2.6763 |

Conclusions

This study provides a complete miss distance analysis of TPN as a bench mark and has some contributions to a systematic way for miss distance analysis of two-point guidance laws. However, our results are valid for a first-order control system without acceleration limit, but the description of its behavior gives more insight to the guidance designers. It is important to note that the worst miss distance of TPN is reduced by increasing the value of the effective navigation ratio due to heading error or step target acceleration (checked for the effective navigation ratio ≤ 20); however, this behavior is not seen for a fifth-order binomial

control system which has a minimum value of 3.75 (or 4.55) due to HE (or step target maneuver).

In addition, an approximate formula is obtained for miss distance budget for a step target maneuver with a random starting time in the presence of seeker noise sources using the curve fitting method. Therefore, an explicit formula is obtained for the optimum effective navigation ratio in order to minimize the RMS miss for a specified value of system time constant. For the optimization with two variables (the effective navigation ratio and system time constant), the above mentioned formula is also preferred to the solving of a transcendental equation in terms of the system time constant. Moreover, an approximate formula for the optimum time constant is derived when the glint noise is the dominant seeker noise source.

Appendix A: MD formulas due to HE

Miss distance formulas are simply written from Eq. (7) or Eq. (8) for integer values of N' due to heading error, that is,

$$\frac{\text{MD}}{-Tv_{M\text{HE}}}\Big|_{N'=2} = e^{-x}Q_2 \quad (\text{A1})$$

$$\frac{2\text{MD}}{-Tv_{M\text{HE}}}\Big|_{N'=3} = -e^{-x}Q_3 \quad (\text{A2})$$

$$\frac{6\text{MD}}{-Tv_{M\text{HE}}}\Big|_{N'=4} = e^{-x}Q_4 \quad (\text{A3})$$

$$\frac{24\text{MD}}{-Tv_{M\text{HE}}}\Big|_{N'=5} = -e^{-x}Q_5 \quad (\text{A4})$$

$$\frac{120\text{MD}}{-Tv_{M\text{HE}}}\Big|_{N'=6} = e^{-x}Q_6 \quad (\text{A5})$$

$$\frac{720\text{MD}}{-Tv_{M\text{HE}}}\Big|_{N'=7} = -e^{-x}Q_7 \quad (\text{A6})$$

$$\frac{5040\text{MD}}{-Tv_{M\text{HE}}}\Big|_{N'=8} = e^{-x}Q_8 \quad (\text{A7})$$

where $x = t_f/T$ and

$$Q_2 = x$$

$$Q_3 = x^2 - 2x$$

$$Q_4 = x^3 - 6x^2 + 6x$$

$$Q_5 = x^4 - 12x^3 + 36x^2 - 24x$$

$$Q_6 = x^5 - 20x^4 + 120x^3 - 240x^2 + 120x \quad (\text{A8})$$

$$Q_7 = x^6 - 30x^5 + 300x^4 - 1200x^3 + 1800x^2 - 720x$$

$$Q_8 = x^7 - 42x^6 + 630x^5 - 4200x^4 + 12600x^3 - 15120x^2 + 5040x$$

Appendix B: MD formulas due to step target maneuver

Miss distance formulas are written from Eq. (9) or Eq. (10) for integer value of N' due to a step target maneuver, that is,

$$\left. \frac{MD}{n_T T^2} \right|_{N'=2} = 1 - e^{-x} G_2 \quad (B1)$$

$$\left. \frac{2MD}{n_T T^2} \right|_{N'=3} = e^{-x} G_3 \quad (B2)$$

$$\left. \frac{6MD}{n_T T^2} \right|_{N'=4} = -e^{-x} G_4 \quad (B3)$$

$$\left. \frac{24MD}{n_T T^2} \right|_{N'=5} = e^{-x} G_5 \quad (B4)$$

$$\left. \frac{120MD}{n_T T^2} \right|_{N'=6} = -e^{-x} G_6 \quad (B5)$$

$$\left. \frac{720MD}{n_T T^2} \right|_{N'=7} = e^{-x} G_7 \quad (B6)$$

$$\left. \frac{5040MD}{n_T T^2} \right|_{N'=8} = -e^{-x} G_8 \quad (B7)$$

where

$$\begin{aligned} G_2 &= x + 1 \\ G_3 &= x^2 \\ G_4 &= x^3 - 3x^2 \\ G_5 &= x^4 - 8x^3 + 12x^2 \\ G_6 &= x^5 - 15x^4 + 60x^3 - 60x^2 \\ G_7 &= x^6 - 24x^5 + 180x^4 - 480x^3 + 360x^2 \\ G_8 &= x^7 - 35x^6 + 420x^5 - 2100x^4 + 4200x^3 - 2520x^2 \end{aligned} \quad (B8)$$

Appendix C: RMS miss formulas due to HE

The mean square miss over the interval $[0 \ t_{f2}]$ is the integral of the t_f -MD² curve divided by t_{f2} . Therefore, the solutions are obtained from Eqs. (A1-A7) for integer values of N' due to a step target maneuver, that is,

$$\left. \frac{RMS \ MD}{Tv_M |HE|} \right|_{N'=2} = \frac{1}{2} \sqrt{\frac{1 + e^{-2x} W_2}{x}} \quad (C1)$$

$$\left. \frac{RMS \ MD}{Tv_M |HE|} \right|_{N'=3} = \frac{1}{4} \sqrt{\frac{1 + e^{-2x} W_3}{x}} \quad (C2)$$

$$\left. \frac{RMS \ MD}{Tv_M |HE|} \right|_{N'=4} = \frac{1}{24} \sqrt{\frac{18 + e^{-2x} W_4}{x}} \quad (C3)$$

$$\left. \frac{RMS \ MD}{Tv_M |HE|} \right|_{N'=5} = \frac{1}{48} \sqrt{\frac{45 + e^{-2x} W_5}{x}} \quad (C4)$$

$$\left. \frac{RMS \ MD}{Tv_M |HE|} \right|_{N'=6} = \frac{1}{480} \sqrt{\frac{3150 + e^{-2x} W_6}{x}} \quad (C5)$$

$$\left. \frac{RMS \ MD}{Tv_M |HE|} \right|_{N'=7} = \frac{1}{2880} \sqrt{\frac{85050 + e^{-2x} W_7}{x}} \quad (C6)$$

$$\left. \frac{RMS \ MD}{Tv_M |HE|} \right|_{N'=8} = \frac{1}{20160} \sqrt{\frac{3274425 + e^{-2x} W_8}{x}} \quad (C7)$$

where

$$\begin{aligned} W_2 &= -2x^2 - 2x - 1 \\ W_3 &= -2x^4 + 4x^3 - 2x^2 - 2x - 1 \\ W_4 &= -8x^6 + 72x^5 - 204x^4 + 168x^3 - 36x^2 - 36x - 18 \\ W_5 &= -2x^8 + 40x^7 - 292x^6 + 948x^5 - 1374x^4 + 708x^3 - 90x^2 - 90x - 45 \\ W_6 &= -8x^{10} + 280x^9 - 3860x^8 + 26800x^7 - 100120x^6 + 198840x^5 - 194100x^4 + 72600x^3 - 6300x^2 - 6300x - 3150 \\ W_7 &= -8x^{12} + 432x^{11} - 9624x^{10} + 115080x^9 - 806940x^8 + 3407760x^7 - 8578440x^6 + 12280680x^5 - 9042300x^4 + 2651400x^3 - 170100x^2 - 170100x - 85050 \\ W_8 &= -8x^{14} + 616x^{13} - 20188x^{12} + 369432x^{11} - 4167324x^{10} + 30208500x^9 - 142431030x^8 + 432792360x^7 - 822173940x^6 + 920358180x^5 - 544083750x^4 + 131109300x^3 - 6548850x^2 - 6548850x - 3274425 \end{aligned} \quad (C8)$$

Appendix D: RMS miss formulas due to step target maneuver with a random starting time

For this case, the RMS miss formulas over the interval $[0 \ t_{f2}]$ are derived as follows:

$$\left. \frac{RMS \ MD}{|n_T| T^2} \right|_{N'=2} = \frac{1}{2} \sqrt{\frac{Z_2}{x}} \quad (D1)$$

$$\left. \frac{\text{RMS MD}}{|n_T| T^2} \right|_{N'=3} = \frac{1}{4} \sqrt{\frac{3 + e^{-2x} Z_3}{x}} \quad (D2)$$

$$\left. \frac{\text{RMS MD}}{|n_T| T^2} \right|_{N'=4} = \frac{1}{24} \sqrt{\frac{18 + e^{-2x} Z_4}{x}} \quad (D3)$$

$$\left. \frac{\text{RMS MD}}{|n_T| T^2} \right|_{N'=5} = \frac{1}{48} \sqrt{\frac{27 + e^{-2x} Z_5}{x}} \quad (D4)$$

$$\left. \frac{\text{RMS MD}}{|n_T| T^2} \right|_{N'=6} = \frac{1}{480} \sqrt{\frac{1350 + e^{-2x} Z_6}{x}} \quad (D5)$$

$$\left. \frac{\text{RMS MD}}{|n_T| T^2} \right|_{N'=7} = \frac{1}{2880} \sqrt{\frac{28350 + e^{-2x} Z_7}{x}} \quad (D6)$$

$$\left. \frac{\text{RMS MD}}{|n_T| T^2} \right|_{N'=8} = \frac{1}{20160} \sqrt{\frac{893025 + e^{-2x} Z_8}{x}} \quad (D7)$$

where

$$\begin{aligned} Z_2 &= e^{-2x}(-2x^2 - 6x - 5) + e^{-x}(8x + 16) + 4x - 11 \\ Z_3 &= -2x^4 - 4x^3 - 6x^2 - 6x - 3 \\ Z_4 &= -8x^6 + 24x^5 - 12x^4 - 24x^3 - 36x^2 - 36x - 18 \\ Z_5 &= -2x^8 + 24x^7 - 92x^6 + 108x^5 - 18x^4 - 36x^3 - 54x^2 \\ &\quad - 54x - 27 \\ Z_6 &= -8x^{10} + 200x^9 - 1860x^8 + 7920x^7 - 15480x^6 \\ &\quad + 11160x^5 - 900x^4 - 1800x^3 - 2700x^2 - 2700x - 1350 \\ Z_7 &= -8x^{12} + 336x^{11} - 5640x^{10} + 48600x^9 - 230580x^8 \\ &\quad + 598320x^7 - 785880x^6 + 407160x^5 - 18900x^4 \\ &\quad - 37800x^3 - 56700x^2 - 56700x - 28350 \\ Z_8 &= -8x^{14} + 504x^{13} - 13244x^{12} + 189336x^{11} - 1613052x^{10} \\ &\quad + 8439060x^9 - 26939430x^8 + 50296680x^7 \\ &\quad - 49753620x^6 + 20083140x^5 - 595350x^4 \\ &\quad - 1190700x^3 - 1786050x^2 - 1786050x \\ &\quad - 893025 \end{aligned} \quad (D8)$$

References

- [1] Nesline, F. W., and Zarchan, P., "Robust Instrumentation Configurations for Homing Missile Flight Control," *Guidance and Control Conference*, August, 1980.
- [2] Nesline, F. W., and Zarchan, P., "Miss Distance Dynamics in Homing Missile," AIAA Paper 1984-1844, Aug. 1984.
- [3] Zarchan, P., "Complete Statistical Analysis of Nonlinear Missile Guidance Systems: SLAM," *Journal of Guidance and Control*, Vol. 2, No. 1, 1979, pp. 71–78.
- [4] Nesline, F. W., and Nesline, M. L., "Wing Size vs Radome Compensation in Aerodynamically Controlled Radar Homing Missiles," *Journal of Guidance, Control and Dynamics*, Vol. 9, No. 6, pp. 645–649, 1986.
- [5] Miwa, S., "Clutter Effect on the Miss Distance of a Radar Homing Missile," *Journal of Guidance, Control and Dynamics*, Vol. 11, No. 4, pp. 336–342, 1988.
- [6] Miwa, S., "Radome Effect on the Miss Distance of a Radar Homing Missile," *Electronics and Communications in Japan*, Part 1, Vol. 81, No. 7, 1998.
- [7] Arabian Arani, A. and Jalali-Naini, S. H., "Approximate Miss Distance Formulas of Proportional Navigation Due to Time Delay Based on Worst Case Analysis," *Aerospace Knowledge and Technology Journal*, Vol. 7, No. 1, pp. 47-62, 2018 (in Persian).
- [8] Zarchan, P., *Tactical and Strategic Missile Guidance*. American Institute of Aeronautics and Astronautics, Inc., 2012.
- [9] Nesline, F. W., and Zarchan, P., "Radome Induced Miss Distance in Aerodynamically Controlled Homing Missiles," *17th Fluid Dynamics, Plasma Dynamics, and Lasers Conference*, June, 1984.
- [10] Alpert, J., "Normalized Analysis of Interceptor Missiles Using the Four-State Optimal Guidance System," *Journal of Guidance, Control, and Dynamics*, Vol. 26, No. 6, pp. 838-845, 2003.
- [11] Bucco, D., Zarchan, P. and Weiss, M., "On Some Issues Concerning the Adjoint Simulation of Guidance Systems," in *AIAA Guidance, Navigation, and Control Conference*, 2012.
- [12] He, T., Chen, W., "A New Interpretation of Adjoint Method in Linear Time-Varying System Analysis," presented at the 2017 IEEE International Conference on Cybernetics and Intelligent Systems (CIS) and IEEE Conference on Robotics, Automation and Mechatronics (RAM), pp. 58-63, 2017.
- [13] Alpert, J., "Adjoint Analysis of Guidance Systems for Time-Series Inputs Using Fourier Analysis," *Journal of Guidance, Control, and Dynamics*, Vol. 43, No. 7, pp. 1359-1364, 2020.
- [14] Donatelli, G. A., and Fleeman, E. L., "Methodology for Predicting Miss Distance for Air Launched Missiles," AIAA 20th Aerospace Sciences Meeting, Florida, 1982.
- [15] Jalali-Naini, S. H., "Noise-Induced Miss Distance Formulas of First-Order Control System Under Proportional Navigation for Arbitrary Navigation Ratios," presented at the 15th International Conference of Iranian Aerospace Society, Tehran, 2016.
- [16] Rusnak, I., "Bounds on the RMS Miss of Radar-Guided Missiles," *Journal of Guidance, Control, and Dynamics*, Vol. 33, No. 6, pp. 1718–1723, 2010.
- [17] Rusnak, I., "Bounds on the RMS Miss of Radar-Guided Missiles Against Sinusoidal Target Maneuvers," *Journal of Guidance, Control, and Dynamics*, Vol. 34, No. 4, pp. 1060–1069, 2011.
- [18] Rusnak, I., "Bounds on the Miss of Radar-Guided Missiles with Discrete Guidance," *Journal of Guidance, Control, and Dynamics*, Vol. 43, No. 4, 2020.

- [19] Rusnak, I., "Bounds on the Miss of Multiple-Model-Based Terminal Guidance Laws," *Journal of Guidance, Control, and Dynamics*, Vol. 38, No. 6, pp. 1001-1011, 2015.
- [20] Jalali-Naini, S. H., Arabian Arani, A., "Proportional Navigation Guidance with Variable Navigation Ratio in Terms of the Angle of Relative Velocity with Respect to Line-of-Sight and its Rate," *Journal of Space Science and Technology*, Vol. 13, Issue. 2, pp. 1-12, 2020 (in Persian)

COPYRIGHTS

©2024 by the authors. Published by Iranian Aerospace Society. This article is an open access article distributed under the terms and conditions of the Creative Commons Attribution 4.0 International (CC BY 4.0) (<https://creativecommons.org/licenses/by/4.0/>).



HOW TO CITE THIS ARTICLE:

S. H. Jalali-Naini, Rahim Asadi, Amir Hossein Mirzaei, "A Comprehensive Miss Distance Analysis of Single-Lag True Proportional Navigation," *Journal of Aerospace Science and Technology*, Vol 17, No 1, 2024, pp. 101-115

DOI: <https://doi.org/10.22034/jast.2024.428886.1170>

URL: https://jast.ias.ir/article_184788.html